

# DEVELOPING TURBULENT FLOWS IN OPEN CHANNELS WITH PILE DIKES

by Fei-Yong CHEN\* and Syunsuke IKEDA\*\*

This paper presents the developing turbulent flow in open channels with pile dikes by using SDS & 2DH turbulence model, in which the formula for the vertical component of the production of turbulence energy due to the bottom friction and the drag of pile dikes is modified. To test performances of the model, calculation examples are illustrated, and the depth-averaged velocities, vertical vorticity, turbulence energy as well as the Reynolds stress are reproduced reasonably well.

**Keywords:** pile dikes, SDS & 2DH turbulence model, turbulence energy, the Reynolds stress, lateral diffusion.

## INTRODUCTION

In fluvial rivers, pile dikes are effective as river training structures. They are used to retard the near-bank flow and protect the river banks, or be used in flood plains to get a balance of lateral sediment transport and maintain channel width not to be changed. Therefore, it is practically meaningful to study the mechanism of flow in open channels with pile dikes.

In 1961, Akikusa et al. treated the retardation by pile dikes<sup>1)</sup>. They considered pile dike region flow and external region flow separately as one dimensional flow, for which the conservation of mass was maintained for the total width. They estimated the longitudinal length of the transition region. It is obvious that the lateral diffusive transport of fluid momentum and suspended sediment plays an important role in this problem. Since Akikusa et al. did not include the effect of lateral diffusion, their model cannot be applied to the practical problems for which the diffusion is predominant. Raupach et al. studied the turbulent flow within vegetation canopies and established a relation between the turbulent shear stress and the local velocity<sup>2)</sup>. Fukuoka et al., based on their experimental data, derived an empirical formula for describing the lateral shear stress acting between the pile dikes region and the center flow region<sup>3)</sup>. On the base of the former studies, Ikeda et al.<sup>4),5),6)</sup> studied the fully developed flow with pile dikes by means of a perturbation method, and provided a mathematical model for determining lateral distributions of fluid velocity and suspended sediment concentration. They also studied experimentally the characteristics of lateral shear stress and sediment transport induced by the lateral diffusivity, and proposed an empirical expression for the lateral eddy viscosity.

Computational modeling is also widely used in river engineering and river mechanics. Nadaoka & Yagi<sup>7),8)</sup> proposed a new turbulence model to calculate the horizontal two-dimensional flow field, and studied the temporal development of horizontal large eddies near the edge of pile dikes. Kanda et al.<sup>9)</sup> investigated the structure of the organized vortex generated at the air-plant interface by using Large Eddy Simulation.

Although some works have been documented on this subject, few studies have been performed on the development of transition region in open channels with pile dikes. The purpose of this paper is to apply the turbulence model developed by Nadaoka & Yagi to analyze the flow in the transition region and to reproduce the distributions of two-dimensional flow field, vorticity distribution, turbulence energy as well as the Reynolds stress.

\* Doctoral Student, Graduate school, Tokyo Institute of Technology (Ookayama 2-12-1, Meguro-ku, Tokyo 152)

\*\* PhD, Professor, Department of Civil Engineering, Tokyo Institute of Technology

## BASIC EQUATIONS

As mentioned in the above, the lateral diffusive transport is mainly of interest in this study. In fact, when the width-to-depth ratio is large, the vertical distribution of flow quantities can be regarded as uniform due to strong vertical mixing induced by the bottom shear. Here we adopt the two-dimensional sub-depth scale (SDS & 2DH) turbulence model developed by Nadaoka & Yagi<sup>(8)</sup> to describe the flow field,

$$\frac{\partial h}{\partial t} + \frac{\partial uh}{\partial x} + \frac{\partial vh}{\partial y} = 0 \quad (1)$$

$$\frac{Du}{Dt} = -g \frac{\partial \eta}{\partial x} - f_x - \frac{c_f}{h} u \sqrt{u^2 + v^2} + \frac{1}{h} \frac{\partial}{\partial x} (2\nu_t h \frac{\partial u}{\partial x} - \frac{2}{3} kh) + \frac{1}{h} \frac{\partial}{\partial y} [\nu_t h (\frac{\partial v}{\partial x} + \frac{\partial u}{\partial y})] \quad (2)$$

$$\frac{Dv}{Dt} = -g \frac{\partial \eta}{\partial y} - f_y - \frac{c_f}{h} v \sqrt{u^2 + v^2} + \frac{1}{h} \frac{\partial}{\partial y} (2\nu_t h \frac{\partial v}{\partial y} - \frac{2}{3} kh) + \frac{1}{h} \frac{\partial}{\partial x} [\nu_t h (\frac{\partial v}{\partial x} + \frac{\partial u}{\partial y})] \quad (3)$$

Eq. 1 is the continuity equation, and Eqs. 2 and 3 are the momentum equations in the longitudinal and the transverse directions,  $x$  and  $y$ , respectively; the depth-averaged velocity components in these directions are  $u$  and  $v$ , respectively. The bed slope is  $s_0$ , the water depth is  $h$ , and the local free surface elevation is  $\eta$ . The symbol  $k$  is the depth-averaged turbulence energy due to the sub-depth scale turbulence,  $\nu_t$  is the depth-averaged eddy viscosity,  $c_f$  is the bottom friction coefficient,  $f_x$  and  $f_y$  are the components of drag force induced by the pile dikes in the directions  $x$  and  $y$ , respectively. According to Raupach & Shaw<sup>(2)</sup>, they are expressed in the following manner:

$$f_x = \frac{ac_d}{2} u \sqrt{u^2 + v^2} \quad (4)$$

$$f_y = \frac{ac_d}{2} v \sqrt{u^2 + v^2} \quad (5)$$

where  $c_d$  is the drag coefficient of a single pile dike, and  $a = d / 2I_x I_y$  is the density of pile dikes, in which  $d$  is the diameter of pile dikes,  $I_x$  and  $I_y$  are the intervals of pile dikes in  $x$  and  $y$  directions, respectively.

The distribution of sub-depth scale turbulence energy,  $k$  in the flow field is determined from the following semi-empirical transport equation:

$$\frac{Dk}{Dt} = \frac{1}{h} \frac{\partial}{\partial x} (h \frac{\nu_t}{\sigma_k} \frac{\partial k}{\partial x}) + \frac{1}{h} \frac{\partial}{\partial y} (h \frac{\nu_t}{\sigma_k} \frac{\partial k}{\partial y}) + p_{kh} + p_{kv} - \epsilon \quad (6)$$

According to the Bossinesq assumption, the depth-averaged eddy viscosity is written as,

$$\nu_t = c_\mu \frac{k^2}{\epsilon} \quad (7a)$$

$$\epsilon = c_\mu^{3/4} \frac{k^{1.5}}{l} \quad (7b)$$

where  $\epsilon$  is the depth-averaged turbulence energy dissipation,  $c_\mu$  (in Eqs. 7a and 7b) and  $\sigma_k$  (in Eq. 6) are empirical constants, and  $l$  is the characteristic turbulence length scale. According to the expression proposed by Nadaoka & Yagi<sup>(8)</sup>, the length scale is correlated to the water depth, such that,

$$l = \alpha h \quad (8)$$

in which  $\alpha$  is a numerical constant.  $p_{kh}$  is the production of turbulence energy induced by the horizontal shear stress, and it can be written as,

$$p_{kh} = \nu_t [2(\frac{\partial u}{\partial x})^2 + 2(\frac{\partial v}{\partial y})^2 + (\frac{\partial u}{\partial y} + \frac{\partial v}{\partial x})^2] \quad (9)$$

$p_{kv}$  is the production of turbulence energy due to the vertical shear stress. For river flows without pile dikes, it is particularly large near the bottom, and it depends strongly on the bottom friction. Rastogi & Rodi<sup>(10)</sup> proposed the following expression for  $p_{kv}$ :

$$p_{kv} = \frac{c_f}{h} (u^2 + v^2)^{1.5} \quad (10)$$

In the present subject, the drag of pile dikes also contributes to  $p_{kv}$ . Considering the effect of retardation induced by pile dikes, Nadaoka & Yagi<sup>(8)</sup> replaced  $c_f/h$  by  $(c_f/h + ac_d/2)$ , and obtained Eq. 11 to modify Eq. 10:

$$p_{kv} = \left( \frac{c_f}{h} + \frac{ac_d}{2} \right) (u^2 + v^2)^{1.5} \quad (11)$$

When we employed Eq. 11 in the fully developed region, it is found that it is not accurate enough as described subsequently.

Since the driving force  $gs_0$  is equal to the resistance to flow at the undisturbed areas outside of the lateral shear layer, we have the following equation:

$$\left[ \frac{c_f}{h} (u^2 + v^2) \right]_{\text{main-flow-region}} = \left[ \left( \frac{c_f}{h} + \frac{ac_d}{2} \right) (u^2 + v^2) \right]_{\text{pile-dike-region}} \quad (12)$$

Considering the equilibrium state, the following relation is derived from the energy balance (Eq. 6):

$$p_{kv} = \epsilon \quad (13)$$

Substituting Eqs. 11 and 12 into Eq. 13, we obtain,

$$\frac{\epsilon_m}{\epsilon_p} = \frac{(\sqrt{u^2 + v^2})_m}{(\sqrt{u^2 + v^2})_p} \quad (14)$$

in which the variables denoted by the subscript "m" are for the main flow region, and "p" for the pile dikes region. As far as the fully developed region is concerned, the flow velocity in the main flow region is much larger than that in the pile dikes region. It is therefore seen from Eq. 14 that the turbulence energy dissipation  $\epsilon_m$  is much larger than  $\epsilon_p$ . It leads to a conclusion that the turbulence energy in the main flow region is much larger than that in the pile dikes region, because  $k$  is proportional to  $\epsilon^{2/3}$  (see Eq. 7b). Hence, when Eq. 11 is employed, the location of the largest value of the turbulence energy at the fully developed region is found to be in the undisturbed area of the main flow region far from the pile dikes. This is apparently incorrect, and Eq. 11 should be modified properly.

Considering the main contribution of the production of turbulence energy due to the vertical velocity gradient, we have,

$$p_{kv} = \frac{1}{h} \int_0^h \tilde{\nu}_t \left( \frac{\partial U}{\partial z} \right)^2 dz \quad (15)$$

in which  $z$  is the vertical coordinate,  $U$  is the composition of the horizontal velocity components at height  $z$  and  $\tilde{\nu}_t$  is the local eddy viscosity. In terms of the shear stress hypothesis proposed by Prandtl<sup>(11)</sup>, the above expression can be correlated to the local kinematic shear stress,  $\tau_t = -u'w'$ , where  $u'$  and  $w'$  are the longitudinal and vertical components of the velocity fluctuations due to the sub-depth scale turbulence, such that,

$$p_{kv} \nu_t = \frac{1}{h} \int_0^h \tilde{\nu}_t \left( \frac{\partial U}{\partial z} \right)^2 dz = \frac{1}{h} \int_0^h \tau_t^2 dz \quad (16)$$

The depth-averaged shear stress can be described by<sup>(2)</sup>,

$$\tau = \tau_b + \tau_d = (c_f + \frac{ac_d h}{2})(u^2 + v^2) \quad (17)$$

where  $\tau_d$  is the shear stress due to pile dikes,  $\tau_b$  is the shear stress due to the bottom friction. Replacing the local shear stress,  $\tau_t$ , in Eq. 16 by the depth-averaged value,  $\tau$ , the following expression is obtained:

$$p_{kv} \nu_t = \frac{1}{h} \int_0^h \tau_t^2 dz = \left[ \left( c_f + \frac{ac_d h}{2} \right) (u^2 + v^2) \right]^2 \quad (18)$$

Since  $\nu_t$  is a function of the depth-averaged turbulence energy, we should eliminate it from Eq. 18 to establish a relation between  $p_{kv}$  and the depth-averaged velocities. Considering Eqs. 13 and 7a, we derive

$$p_{kv} \nu_t = \nu_t \epsilon = c_\mu k^2$$

From the above expression and Eq. 18, a formula for  $k$  is reduced to

$$k = \left( c_f + \frac{ac_d h}{2} \right) (u^2 + v^2) / c_\mu^{1/2} \quad (19)$$

A combination of Eqs. 7, 13 and 19 yields

$$p_{kv} = \left[ \left( c_f + \frac{ac_d h}{2} \right) (u^2 + v^2) \right]^{1.5} / l \quad (20)$$

Assuming the vertical velocity distribution takes a similar profile everywhere, Eq. 20 is applied to the transition area.

## COMPUTATION

Eqs. 1-3, together with Eq. 6, constitute a complete set that can be used to solve the distributions of velocity components and turbulence energy. The boundary conditions should be specified on the river banks, and at the inlet cross-section as well as the outlet cross-section. Obviously, the river banks exert frictional forces on the flow, and the velocities on the walls are zero. The effect of the walls are, however, neglected herein, because the ratio of the width to the depth is assumed to be large, and therefore a slip condition is adopted on the river banks.

The numerical constants,  $c_\mu$ ,  $\sigma_k$  and  $\alpha$  are taken to be 0.09, 1.0 and 0.1, respectively. The initial conditions are calculated from a simplified model which assumes that the eddy viscosity is constant everywhere in Eqs. 2 and 3. The periodic conditions are chosen for the inlet boundary, and the first order derivative of the variables in the x-direction is taken to be zero at the outlet boundary. Other flow parameters are determined according to the experiments performed by Ikeda et al. ([5], Run 1) and Tsujimoto et al.([12], Run B1), which are defined as Case 1 and Case 2, respectively.

**Table 1: Major Parameters for Calculation**

	width of channel B(cm)	length of channel L(cm)	water depth h(cm)	bed slope $s_0$	friction coefficient $c_f$	drag coeff. of pile dikes $c_d$	pile-dikes region width $B_s$ (cm)	density of pile-dikes $a$ (cm <sup>-1</sup> )
Case 1	96	1250	6	0.001	0.007	1.8	30	0.01
Case 2	40	1500	4.28	0.00149	0.004	2.9	12	0.019

### VELOCITY PROFILES

Fig. 1 shows the depth-averaged horizontal flow field of Case 1, which is calculated by the numerical model described in the above. It indicates that the flow is retarded in the pile dikes region ( $x$ : 500-1250 cm,  $y$ : 0-30 cm) and a transition region with strong lateral diffusion is generated. It is seen that some distance(from  $x$ =500 to about  $x$ =900 cm) is required to reach a fully-developed region. For the transition region, the computed velocity profiles in some cross-sections are shown in Fig. 2 to compare with the existing experimental data (Case 1). Since the width of channel is not large enough, the lateral diffusion affects the whole main flow region; i.e. the main flow is accelerated as the flow in the pile dikes region is decelerated. The comparison of velocity profiles between the calculated results and the experimental data shows a good agreement.

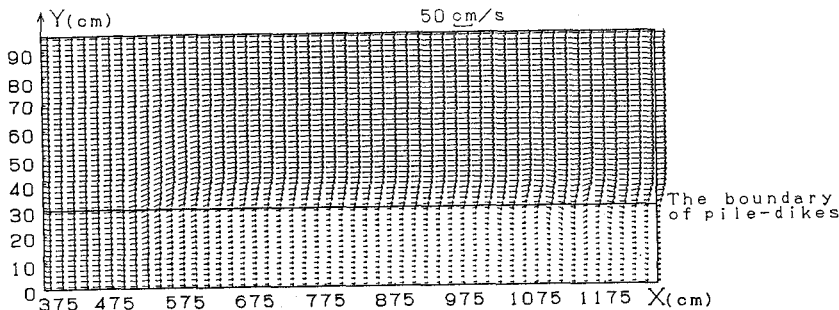


**Fig. 1 An instantaneous flow field at  $t$ =33 second (Case 1)**

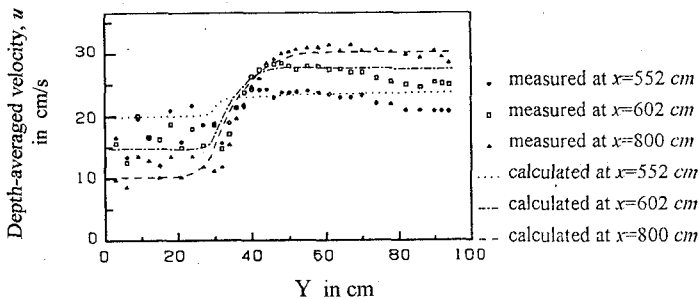


**Fig. 2 Comparison of the calculated velocity with the existing experimental data (Case 1)**

### VORTICITY

For Case 2, Figs. 3-5 illustrate the instantaneous vorticity distributions at 30, 40, 50 seconds from the start of calculation, respectively. In the inlet section ( $x = 0 \sim 450$  cm), no vorticity source exists on the horizontal plane, because we adopt the non-slip condition for the river banks, and a uniform inflow condition for the inlet boundary. Hence, as shown in the figures, the vertical vorticity does not exist in the inlet section. On the contrary, the pile dikes induce retardation to the flow, and a difference of flow velocity is generated at the interface between the pile-dike region and the main flow region. This is the source of vorticity.

It is seen that the vorticity field begins to fluctuate at about  $x=820$  cm, suggesting to roll up to discrete vorticities. This is spatially developing instability in the down-stream direction. As shown in Figs. 3-5, the longitudinal scale of the large eddies in this region reaches to about 75 cm. The period of vorticity is about 3.1 seconds.

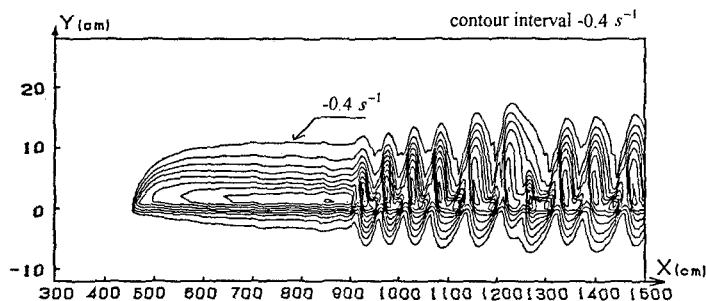


Fig. 3 The instantaneous distribution of vorticity at  $t=30$  second (Case 2)

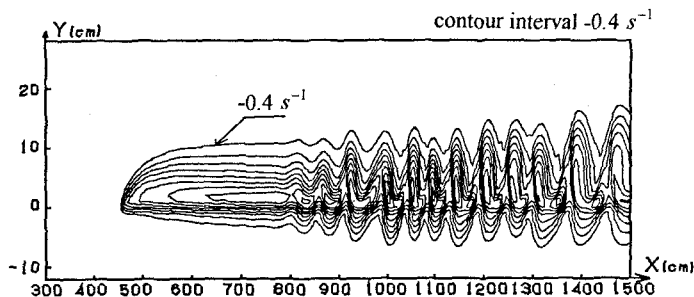


Fig. 4 The instantaneous distribution of vorticity at  $t=40$  second (Case 2)

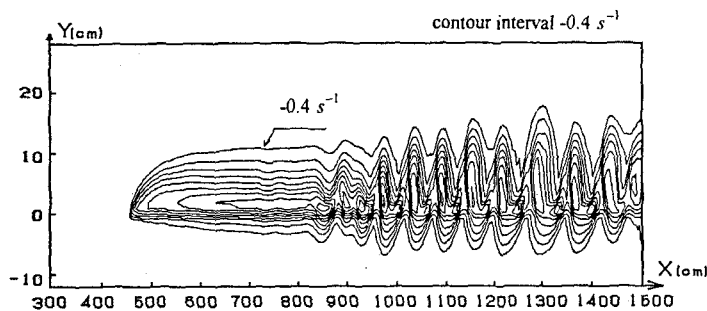


Fig. 5 The instantaneous distribution of vorticity at  $t=50$  second (Case 2)

## TURBULENCE ENERGY AND THE REYNOLDS STRESS

By substituting Eq. 20 into Eq. 6, the SDS turbulence energy distribution is solved. In the fully developed region the peak value of the turbulence energy in a cross-section exists near the boundary of the main flow region and the pile-dikes region (see Fig. 6). The turbulence energy (the vertical component is not included, because it was not measured by Tsujimoto) is compared with the measurement (Case 2). The predicted profile is similar. However, the absolute values of the prediction are slightly larger than the measurement. In Fig. 6,  $u'_L$  and  $v'_L$  are the components of velocity fluctuation due to the horizontal large eddies, and  $k$  is the sub-depth scale homogenous turbulence energy.

The computed distribution of the Reynolds stress component,  $-\overline{u'v'}$ , in fully developed region is compared with the measured data (Case 2) in Fig. 7. The skewed distribution is reasonably reproduced, and the peak value of the Reynolds stress agrees with the measurement.

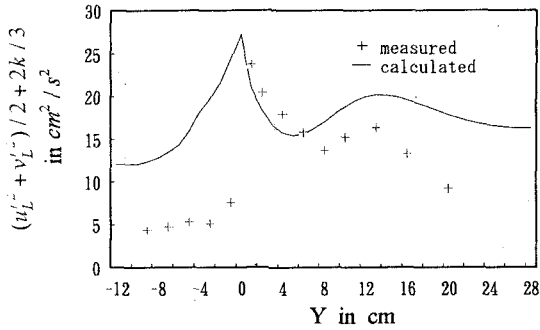


Fig. 6 Comparisons of the turbulence energy (case 2)

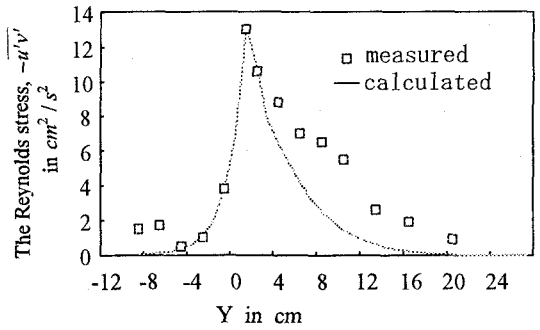


Fig. 7 Comparisons of the Reynolds stress (Case 2)

## CONCLUSIONS

This paper employed SDS & 2DH turbulence model to represent the turbulent flow in open channels with pile dikes. The velocity and vorticity distributions were reproduced reasonably well.

This paper modified the expression for the vertical production of turbulent energy due to the vertical shear stress induced by the bottom friction and the drag of pile dikes. By using this formula, a reasonable distribution of turbulence energy was obtained.

The calculated velocity profiles, the lateral distributions of the Reynolds stress and the turbulence energy were tested by the existing experimental data. The results are found to be reasonable.

## ACKNOWLEDGMENT

Thanks are due to Dr. H. Yagi, lecturer of Tokyo Institute of Technology (TIT), and Dr. N. Izumi, research associate of TIT, by whom valuable suggestions were provided to the first author.

## REFERENCES

1. I. Akikusa, H. Kikkawa, Y. Sakagami, K. Ashida, and A. Tsuchiya (1961) Study on dikes, *Report of Public Works Res. Inst.*, Ministry of Construction of Japan, Tokyo, Japan, Vol. 107, pp.61-153, (in Japanese).
2. M. R. Raupach and R. H. Shaw (1982) Averaging procedures for flow within vegetation canopies, *Boundary-Layer Meteorology*, Vol.22, pp.79-90.
3. S. Fukuoka and K. Fujita (1989) Added flow resistance of flood flow due to lateral velocity discontinuity, *Proc. 33rd Japanese Conf. on Hydr.*, JSCE, Tokyo, Japan, pp.325-330, (in Japanese).
4. S. Ikeda, N. Izumi and R. Ito (1991) Effect of pile dikes on flow retardation and sediment transport, *J. of Hydraulic Engineering*, ASCE, Vol. 117, No. 11, pp.1459-1478.
5. S. Ikeda, K. Ohta and H. Hasegawa (1992) Periodic vortices at the boundary of vegetated area along river bank, *Proc. of JSCE*, No.443, pp.47-54, (in Japanese).
6. S. Ikeda, K. Ohta and H. Hasegawa (1992) Effect of bank vegetation on flow and sediment deposition, *Proc. of JSCE*, No.447, pp.25-34, (in Japanese).
7. K. Nadaoka and H. Yagi (1993) A turbulent model for shallow water and its application to large-eddy computation of longshore currents, *Proc. of JSCE*, No.473, pp.25-34, (in Japanese).
8. K. Nadaoka and H. Yagi (1993) Horizontal large-eddy computation of river flow with transverse shear by SDS & 2DH model, *Proc. of JSCE*, No. 473, pp.35-44, (in Japanese).
9. M. Kanda, S. Inagaki and M. Hino (1993) Large eddy simulation of organized structure and momentum transfer within and above a plant canopy, *Proc. of JSCE*, No.461, pp.39-48, (in Japanese).
10. A. K. Rastogi and W. Rodi (1978) Predications of heat and mass transfer in open channels, *J. of Hydraulic Division*, ASCE, Vol.104, pp.397-420.
11. B. E. Launder and D. B. Spalding (1972) Lectures in mathematical models of turbulence, *Academic Press*, London and New York.
12. T. Tsujimoto and T. Kitamura (1994) Experimental study of transverse mixing in open-channel flow with longitudinal zone of vegetation along side wall, *Proc. of JSCE*, No.491, pp.61-70, (in Japanese).